3 Biotech (2017) 7:312
DOI 10.1007/s13205-017-0919-y

ORIGINAL ARTICLE

A highly sensitive electrochemical biosensor based on AuNP-modified gold electrodes for selective determination of serum levels of crosslaps

Patricia Khashayar[1,2,3] · Ghassem Amoabediny[4,5] · Bagher Larijani[6] · Morteza Hosseini[1] · Rik Verplancke[2] · Michel De Keersmaecker[7] · Annemie Adriaens[7] · Stefan Goemaere[8] · Tom Fiers[8] · Jan Vanfleteren[2]

Received: 17 February 2017 / Accepted: 16 August 2017

Abstract This article explains a step-wise protocol to develop an electrochemical sensor to quantify serum levels of C-telopeptide (CTX) crosslinks also known as crosslaps in a matter of minutes and with high level of accuracy. The technique needs only one-step (incubation) and can thus be used for point of care screening. Due to the excellent electrical properties of the as-prepared immunosensor, CTX levels were successfully measured from 1 to 1000 pg/mL. This is while the normal reference of the marker is 50–450 pg/mL, suggesting that the sensor can acceptably detect CTX. The results also showed a good correlation with ECLIA in measuring serum levels of CTX.

Keywords CTX · Biosensor · Bone turnover marker · Electrochemistry · Crosslaps

✉ Bagher Larijani
larijanib@tums.ac.ir

[1] Nanobiotechnology Department, Faculty of New Sciences and Technologies, University of Tehran, Tehran, Iran

[2] Center for Microsystems Technology, IMEC and Ghent University, Zwijnaarde, Ghent, Belgium

[3] Osteoporosis Research Center, Endocrinology and Metabolism Clinical Sciences Institute, Tehran University of Medical Sciences, Tehran, Iran

[4] Department of Biotechnology, Faculty of Chemical Engineering, School of Engineering, University of Tehran, Tehran, Iran

[5] Nanobiotechnology Department, Research Center for New Technology in Life Sciences Engineering, University of Tehran, Tehran, Iran

[6] Endocrinology and Metabolism Research Center, Endocrinology and Metabolism Clinical Sciences Institute (EMRI), Shariati Hospital, Tehran University of Medical Sciences, Kargar St., Tehran, Iran

[7] Department of Analytical Chemistry, Ghent University, Krijgslaan 281 (S12), Ghent, Belgium

[8] Unit for Osteoporosis and Metabolic Bone Diseases, Ghent University Hospital, Ghent, Belgium

Introduction

Osteoporosis, characterized by low bone mineral density (BMD) and micro-architectural deterioration of bone tissue, is the common cause of bone fragility and fracture. With the upsurge of life expectancy, the number of individuals diagnosed with osteoporosis and its complications is increasing in every geographical region, and the incidence of hip fracture is estimated to rise from 1.66 million in 1990 to 6.26 million by 2050 (Dhanwal et al. 2011; Khashayar et al. 2010). The economic burden of fragility fractures in the European Union is estimated to be at 37 billion, and is expected to increase by 25% in 2025 (Svedbom et al. 2013). Considering the increasing number and heavy burden of osteoporotic fractures and the associated morbidity, considerable effort has been made for early detection of osteoporosis, aggressive fracture prevention, and monitoring of patients at high risk of fractures (Johnell and Kanis 2006). At the time being, BMD measurement using dual energy X-ray absorptiometry (DXA) is routinely used for the diagnosis of osteoporosis (Nishizawa et al. 2012; Imai 2014). This is while about 50% of postmenopausal women with history of fracture have normal BMD levels (Sornay-Rendu et al. 2005).

More recent studies, therefore, have emphasized on the use of bone turnover markers (BTMs) in clinical evaluation of bone quality, fracture risk assessment, and drug efficacy studies (Heaney et al. 2003; Khashayar et al. 2015;

Published online: 13 September 2017

Srivastava et al. 2005). According to these studies, BTMs, especially resorption markers, are an independent predictor of fracture risk, in addition to BMD.

Type I collagen accounts for 90% of the organic matrix of the bone, and is subjected to a series of enzymatic and non-enzymatic intra- and extracellular post-translational modifications that may induce bone strength during the normal aging process or on the pace of a disease (Garnero 2012). Collagen crosslinking is, therefore, of great importance in determining the biomechanical competence of the bone (Vasikaran et al. 2011). Several studies have related the bone content of C-telopeptide (CTX) crosslinks also known as crosslaps, in part independent of the bone mineral value, with bone strength. They, therefore, suggest serum CTX as a reference bone resorption marker (Chubb 2012; Baim and Miller 2009). In other words, despite the marked effects of circadian variation and other factors such as diet on serum levels of CTX, the marker is reported to be sensitive to short-term changes in bone metabolism.

The first serum CTX assay was a competitive polyclonal antibody enzyme-linked immunosorbent assay (ELISA) (Bonde et al. 1997; Rosenquist et al. 1998). This is while apart from analytical variability, ELISA is expensive, time-consuming, and not always available. Biosensors, on the other hand, can help determine reaction kinetics of marker interaction in real time rapidly. The technique needs only one step (incubation) and can thus be used for point of care screening (Hannon et al. 1999; Wang 2006). In the past years, several attempts have been made to develop a label-free immunosensing biosensor for the detection of CTX levels, none of which has become commercialized (Yun et al. 2009; Kim et al. 2013; Park et al. 2015; Ramanathan et al. 2016; Afsarimanesh et al. 2017). The majority of these biosensors are based on sandwich and or optical assays.

This article explains a step-wise protocol to develop a label-free electrochemical sensor to quantify serum levels of CTX in a matter of minutes and with high level of accuracy (Khashayar 2017).

Experimental procedures

Chemicals and materials

Bovine Serum Albumins (BSA), Tween 20, b-1-ethyl-3-(3-dimethylamonipropyl) carbodiimide (EDC), sulfo- *N*-hydroxysuccinimide (sulfo-NHS), L-glutathione reduced (GSH), and potassium hexacyanoferrate (III) ($K_3Fe(CN)_6$) were purchased from Sigma-Aldrich. EDC and sulfo-NHS were dissolved in water at 0.4 M and 0.1 M, divided into small aliquots, and stored at −20 °C. Phosphate-buffered saline (PBS) solution (10 mM, NaCl 0.138 M, KCl 0.0027, pH 7.4, 25°) and PBS-Tween 20 were purchased in powder form from Sigma-Aldrich, and prepared by dissolving 1 package in 1000 mL of de-ionized (DI) water.

Anti-collagen type I antibody (MAB1340) and Human Collagen type I (CC050) were obtained from Merck Chemicals (Belgium). These two components were reconstituted in PBS buffer. All solutions, including Ab conjugates, sulfo-NHS and EDC, were used within 24 h of preparation. The clinical serum samples were obtained from the Endocrinology and Metabolism Research Institute. All the experiments were carried out at room temperature.

Apparatus

The electrochemical measurements were performed with Autolab PGSTAT101 (Metrohm, The Netherlands). They were carried out in 0.1 mM $K_3[Fe(CN)_6]$, containing 0.01 M NaCl, at room temperature (23 °C), using the three-electrode configuration fabricated in our laboratory according to the procedure described elsewhere (Khashayar et al. 2016). A common method of electrochemical testing begins with a cyclic voltammogram (CV) in order to determine the formal potential of the electrochemical sensor for differential pulse voltammetry (DPV). The CV and DPV measurements were performed to control electrode modification steps and to quantify the target molecule concentration at the sample surface, respectively. The CV potential was cycled from 0.0 to 1.2 V with scan rate 0.1 V/s. The DPV measurements were performed in $[FeCN_6]^{3-/4-}$ applying the following parameters: 0.025 V modulation amplitude, 0.05 s modulation time, 0.005 step potential, and voltage range from 0.5 to 1.1 V.

A slightly different offset is reported between the working and reference electrodes in sensors with individualized quasi-reference electrodes (Uludag et al. 2014). As a result, the peaks of DPV plots were averaged to obtain formal potential of our 3-electrode system.

Calibration curves were obtained based on triplicate measurements and parameters such as lower limits of detection (LLD), upper limits of detection (ULD), and consequently a dynamic range were calculated. Other assessed parameters included limit of detection (LOD) and limit of quantification (LOQ), sensitivity (slope of the gradient), reproducibility (standard deviation divided by the average in percent), tightness of fit (*R*-square of trend line applied), and behavior (liner, non-linear, etc.). LOD is the lowest concentration of the analyte, which gives an analytical signal greater than the background value plus 3* standard deviation.

Scanning transmission electron microscopy (STEM), (JeolZeiss—EM10C JEM-2200FS FEG (S)TEM)—80 operated under high tension of 200 kV) was used to collect

information for visualization on the prepared gold nanoparticles and to test for their ability to bind with the proteins. A high-angle annular dark field (HAADF) detector was used to distinguish the smallest and dispersed prepared gold nanoparticles from the porous gold substrate. The bright field detector (BF) was used to visualize lager prepared nanoparticles.

X-ray photoelectron spectroscopy (XPS) was performed with an electron spectrometer (SSI-SSX100) to estimate the composition of the surface and confirm successful immobilization in each step.

In order to check the accuracy of the sensor, the electrochemiluminescence immunoassay (ECLIA, Elecsys 2010 autoanalyzer, Roche Diagnostics GmbH, Germany) was used to measure the serum levels of CTX (Intermediate precision CV of <20%).

Fabrication of immunosensor

Preparation of gold electrode array

The glass slide patterned with gold microelectrodes was fabricated according to the method reported elsewhere (Khashayar et al. 2016). Briefly, each substrate consisted of gold reference (RE), counter (CE), and working electrodes (WE). A layer of SU-8 photoresist was later used as an insulation layer to cover the whole surface, exposing just the electrodes to the electrolyte solutions (Fig. 1). A common printed circuit board (PCB) with electrical connection leads and lines to the electrodes was used to connect the array to the potentiostat.

The electrodes were cleaned, just before the electrodeposition step, in 0.5 M H_2SO_4 (external Ag/AgCl reference electrode and Pt counter electrode, in situ gold electrode as working electrode). This step was conducted in the potential range of 0.0–1.5 V at a scan rate of 0.1 V/s. 20 cycles were needed to obtain reproducible CVs, suggestive of a clean gold surface. After finishing the electrochemical pre-treatment step, the electrodes were washed with DI water.

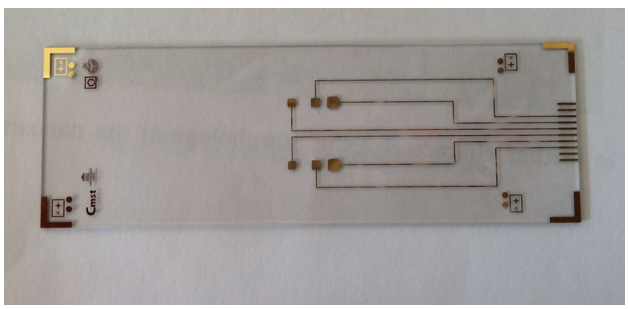

Fig. 1 A picture of the fabricated electrode

In order to coat the working electrode with a gold nanoparticle layer that would allow sufficient immobilization of antibodies on the surface in later steps, the CV-electrodeposition technique (scanning potential of 0.0–1.5 V at a scan rate 0.1 V/s for 100 scans in an aqueous solution of 1.0 mM $HAuCl_4$ and 0.01 M H_2SO_4 in the presence of 0.01 M NaCl via external Ag/AgCl reference electrode and Pt counter electrode) was used (Khashayar et al. 2016). It should be noted that in this way the surface was coated with nanoclusters of AuNPs, which for simplicity are referred to as AuNPs in the rest of the article.

Immobilization

The immunosensor was fabricated by the immobilization of antibodies on the modified gold electrode array through EDC/NHS covalent-linking. First, 4 µL of a 10-mM GSH solution was disposed on the working electrode and dried at room temperature for 1 h. After gently rinsing with distilled water, the gold electrodes functionalized with carboxylic groups were incubated in a mixture solution of 400 mM EDC, 100 mM Sulfo-NHS, and 10 µg/mL CTX for 2.5 h. In order to make this solution, EDC and sulfo-NHS were first reacted with each other for 20 min and then the CTX Ab was added to the solution and incubated for another 60 min. The zero-cross length linkers such as EDC/NHS facilitate the attachment of the carboxylic acid groups of the GSH-modified electrode to the amine group in the antibody solution. Subsequently, the electrodes were rinsed with PBS to remove the excess antibody complex.

In order to avoid non-specific binding, 10 µL of BSA solution (0.2% m/v in 0.1 M PBS, pH 7.4) was deposited on each electrode for 1 h. Finally, the electrodes were rinsed with 0.1 M PBS (Coupling Buffer) and 0.1 M PBS-Tween 20 (Washing Buffer). PBS-Tween 20 is commonly used to minimize the background noise from non-specific binding in bioassays. The electrodes were then shaken to remove excess water. The electrodes carrying the conjugated antibodies were treated carefully as the detachment of the conjugates can be troublesome if proper handling/pipetting is not applied during washing/blocking steps. Fully modified electrodes were stored dry until further use but not longer than 1 day.

Results and discussion

There are numerous methods for rapid and quantitative measurement of clinically important analytes. From among them, immunosensor assays have the capability for rapid and specific detection of biomarkers in biological samples, including serum (Holford et al. 2012). The relative lack of long-term stability of biological molecules on the surface,

however, is the most serious limitation in commercializing such biosensors and in their routine use in clinical practice (Omidfar et al. 2013).

Currently, noble metal surfaces, particularly gold nanoparticles (AuNPs), are considered as ideal supports for the fabrication of electrochemical sensors because of their superior stability, high surface-to-volume ratio, protein-friendly environment, capacity for surface modification, and complete recovery in biochemical redox processes (Vastarella et al. 2007; Shamsipur et al. 2014). In this work, a novel gold electrode array was successfully prepared based on in situ electrodeposition of AuNPs on gold surface followed by immobilization of antibodies. The in situ deposition of high-content AuNPs on the gold surface not only provided a simple and controllable method for the electrode preparation but also amplified electron transfer and signal response of immuno-recognition events.

Assessment of surface morphology of modified electrodes

Once immobilized on the surface, biomolecules adsorbed on AuNPs are not free anymore and adopt a specific conformation. This results in a more rigid protein structure, compared with when the molecule was able to change its orientation and conformation rather freely in solution. This raises the question of how the activity of an antibody is affected after conjugation with a gold particle.

Although protein-conjugated gold nanoparticles have been successfully employed as biological markers for decades, instances of total or partial loss of specific activity of the protein upon conjugation have been reported (La Belle et al. 2013).

We used STEM to determine the three-dimensional surface morphology of the electrodes after every modification step and to study the interaction between CTX antibody and the electrode surface.

STEM images of the fabricated AuNPs on gold surface (Fig. 2) demonstrated that the electrodeposition resulted in surfaces with highly uniform AuNP distribution. The fabricated AuNP were approximately $\sim$20 nm in diameter. As a result, the presence of large number of uniform AuNPs on the electrode resulted in the increment of the total surface roughness, and thus surface area of the electrode (as reported in our previous article (Khashayar et al. 2016). The study of the Ab-functionalized electrodes revealed the affinity of AuNPs to the CTX antibody and the aggregation properties of the resulted antibody complex.

Current transient of AuNP-modified gold electrodes

The AuNP layer enhanced the electrochemical conductivity of the modified electrode compared to the bare one, which is related to the increased electrode's active surface area (Fig. 2). The real electrochemical surface area of the gold electrodes was calculated to be 2.3 times greater than the area before electrodeposition, providing a bigger surface for antibody immobilization. In addition, it showed a remarkable oxidation peak at 0.142 V and a reduction peak at 0.9 V was reported after electrodeposition. This sharp oxidation peak is due to oxide formation and the occurrence of Au stripping. Therefore, the AuNP-modified electrode displayed an advantage for signal amplification.

After the addition of the antibody complex, however, a significant signal reduction in electrical response was noted. This is due to the formation of a hydrophobic layer after the binding of antibody on the electrode surface, which retards the interfacial electron transfer and is reflected as reduced electrical response.

Analytical procedure

The fundamental structural unit of an antibody is two identical heavy and light chains interconnected by disulfide bridges. The chains are entirely composed of constant and variable regions, combining one interaction site for the antigen. The conformation of amino acids of antibody in this site determines its antigen binding activity (Killard et al. 1995). Several non-covalent bonding, such as van der Waals and non-polar hydrophobic interactions as well as London dispersion attractive and steric repulsion forces contribute to the molecular interactions between the antibody and antigen.

The antibody–antigen reaction on our electrodes was tested by the introduction of Ag solution using a fine pipette. In this regard, concentration gradients of the target, CTX, were prepared and run against the sensor for verification. The concentration against current read during DPV analysis was used to calculate and plot linear and logarithmic fit R-squares (degree of fit).

Under the optimum conditions, the DPV peak current of the immunosensor array decreased proportionally with the increasing concentration of CTX analytes (Fig. 3). A logarithmic response curve with a slope of 0.004 and a linear regression constant (R^2) of 0.96 was observed over the tested concentration range (1–1000 pg/mL) (Fig. 4). The correlation coefficient was 0.82 and the LOQ was calculated to be 16.5. The LOD was estimated to be 5.44 pg/mL, which was much lower than the normal CTX range in plasma (50–450 pg/mL), indicating the sensitivity of the assay.

Optimization

Several factors affect the LOD and thus the sensitivity of an assay. Reducing the risk of antibody losing its activity

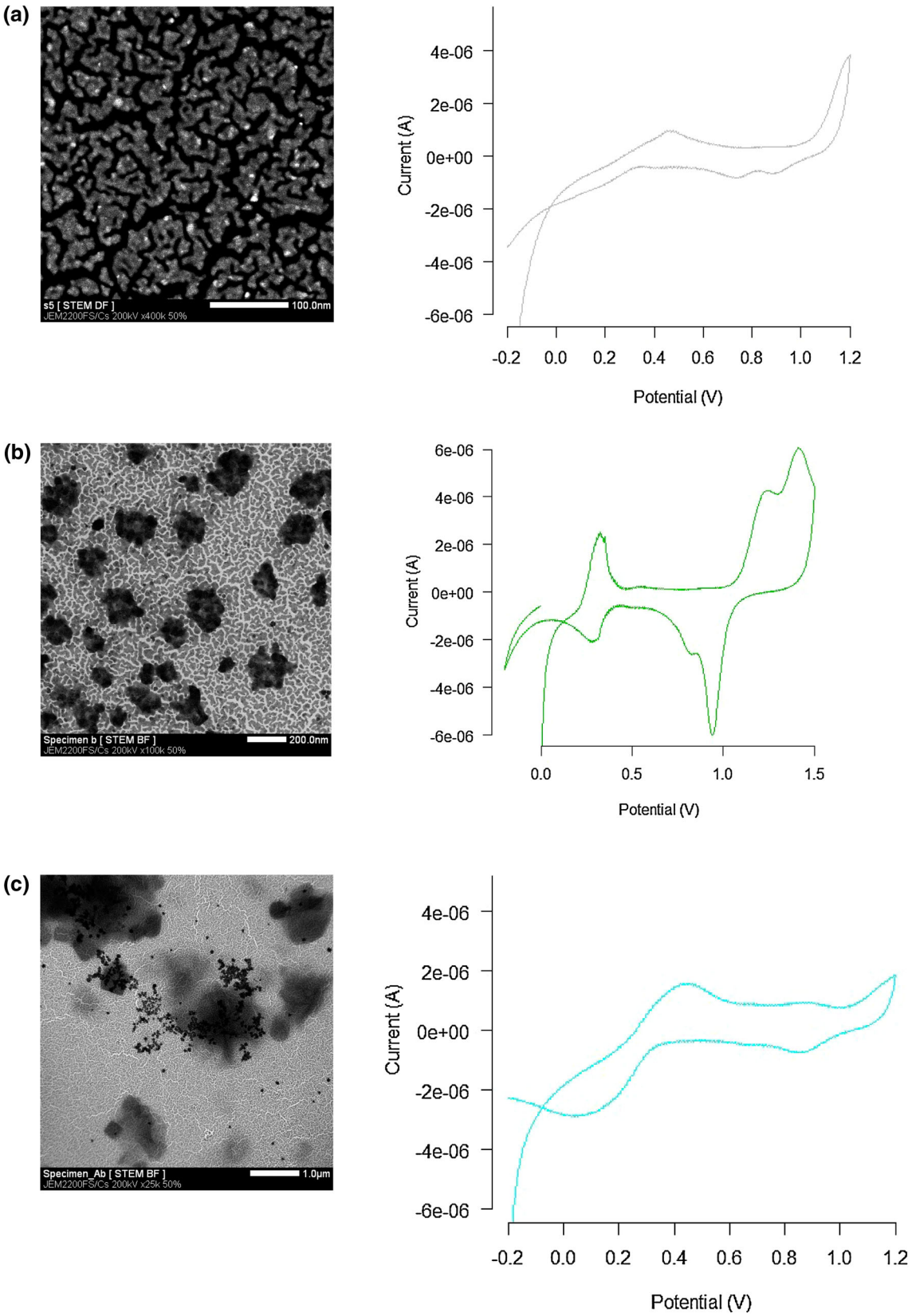

Fig. 2 **a** STEM results micrographs and **b** cyclic voltammogram (in 0.1 mM $K_3[Fe(CN)_6]$, containing 0.01 M NaCl, at room temperature (23 °C) from 0.0 to 1.2 V with scan rate 0.1 V/s) of **a** bare gold, and **b** AuNP-modified **c** Ab-functionalized electrode (Khashayar 2017)

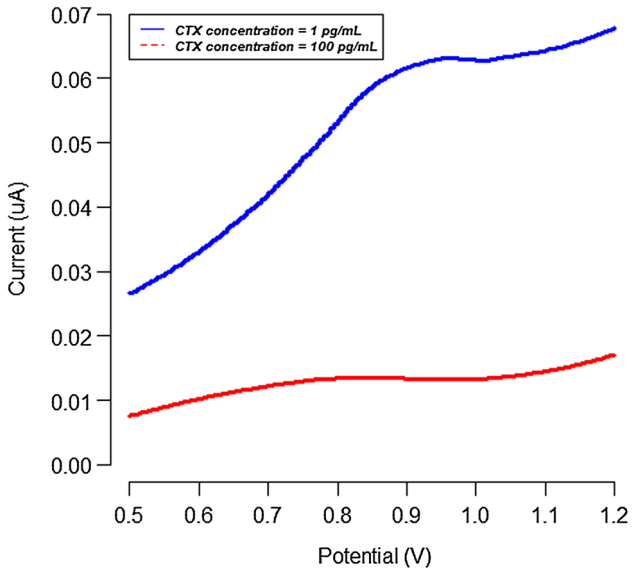

Fig. 3 DPV (in 0.1 mM $K_3[Fe(CN)_6]$, containing 0.01 M NaCl, at room temperature (23 °C) with 0.025 V modulation amplitude, 0.05 s modulation time, 0.005 step potential, and voltage range from 0.5 to 1.1 V) of 1 pg/mL (lowest) and 100 pg/mL concentrations of CTX antigen

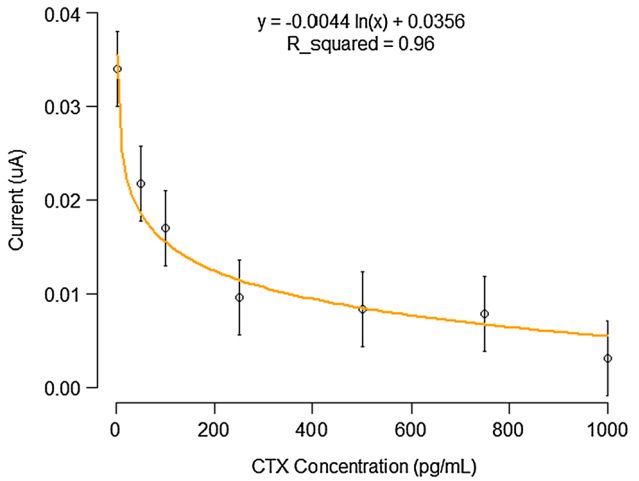

Fig. 4 Calibration curve of different CTX concentrations using the proposed immunosensor for signal tracing and amplification (Khashayar 2017)

upon conjugation and nonspecific binding can help in this regard. The morphology of the electrode's surface, influenced by factors such as surface roughness, can also affect the intensity of the analytical signal.

In this study, we tried to improve the Ab immobilization process through modifying the electrode surface with AuNPs and cross-linkers. Nonspecific binding was reduced through uniform distribution of AuNPs on the electrode surface.

As a result, the amount of immobilized antibodies, their proper conjugation to the surface, and improved response signal depend on the amount and size of AuNPs deposited on the surface. The latter is related to the deposition time and scan rate. Due to geometrical considerations, the application of AuNPs of ~20 nm is shown to lower the sterically hindered binding of proteins on suitable sites of gold (German et al. 2014). The successful deposition of AuNPs with the suitable size on the surface was achieved in the previous study by the same group (Khashayar et al. 2016).

A schematic illustration of the preparation process of the immunosensor is shown in Fig. 5. Factors such as the concentration of GSH and Ab as well as the sulfo-NHS:EDC concentration and ratio were studied through a design of experiments (DOE) where a series of concentrations were tested against each other to obtain the largest signal to noise ratio from the assay. Optimum concentration was found to be 10 mM for GSH; 400 mM for EDC: 100 mM for sulfo-NHS, and 10 µg/mL for Ab. A 1:1:1 ratio for EDC, NHS, and Ab was considered as the optimum concentration for the antibody complex.

The incubation time is another important parameter affecting the analytical performance of the immunoassay. At room temperature, the stripping voltammetric response improved with the increasing incubation time following the antibody complex immobilization and then tended to constant values after 2.5 h. Similar trend was noted after the reaction time between the Ab and Ag was increased to 80 s. This showed the saturated binding between the AuNPs and the antibody as well as between the analyte (antigen) and antibody on electrode surface. Therefore, an incubation time of 2.5 h and a reaction time of 80 s were selected for the immunosensor.

As mentioned in the literature, environmental factors such as temperature and pH also play an important role in the immobilization efficiency. Not only hydrogen bonds are reported to be more stable at low temperature, but also antibodies and antigens are reported to be more stable at these temperatures (Reverberi and Reverberi 2007). As no significant change was reported in our results when the tests were performed at different temperatures (4 °C—room temperature), all the steps were performed at room temperature. The highest activity of the sensor was observed at pH 4.5, in which all the used material (sulfo-NHS, EDC and GSH as well as the antibody) are reported to have the best functionality (Fischer 2010; Hormozi-Nezhada et al. 2012).

Evaluation of specificity, cross-reactivity, and cross-talk

To investigate the specificity and cross-reactivity between analytes and Ab-functionalized surface, the DPV results of the immunosensor array incubated with CTX,

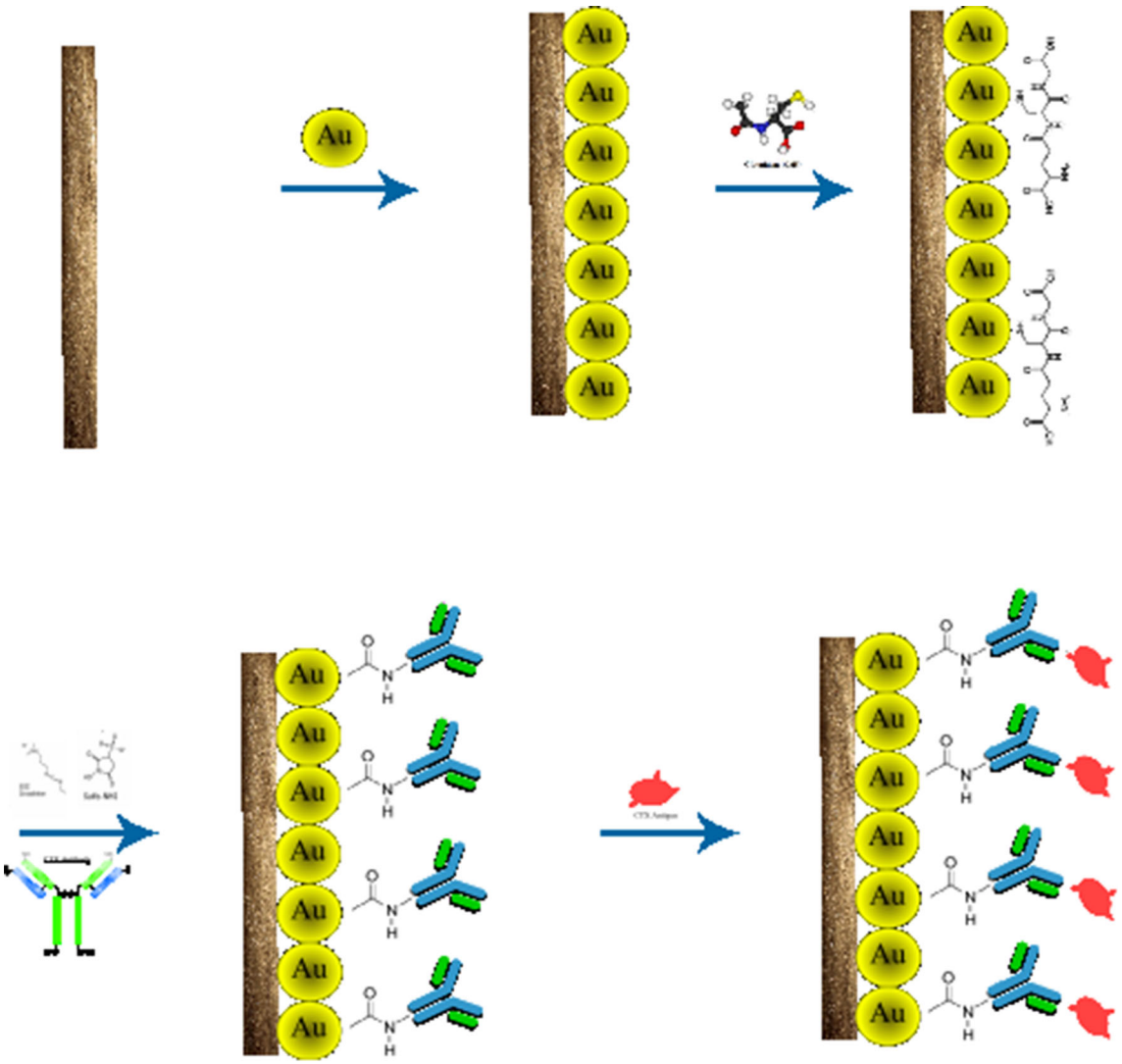

Fig. 5 Surface preparation is typically made possible by modifying the gold surface by AuNP, leaving carboxyl groups on the surface which in turn can be activated using zero crosslength linkers such as (EDC/NHS), rapidly accepting an antibody, and detection can occur under target binding (Khashayar 2017)

Osteocalcin, and PTH were compared. As expected, the immunosensor responded only toward its corresponding proteins. Apparently, the cross-reactivity in the array was negligible (a minimum change of <3% from baseline value), which can be attributed to efficient blocking of nonspecific binding sites on gold (Fig. 6).

In this work, as the Ab complex was immobilized on AuNPs, the Ab–antigen reaction would only accumulate on the AuNPs, resulting in a localized stripping reaction at the individual electrode. Hence, the possible cross talk, which generally results from the diffusion of electroactive indicator produced on one electrode to neighboring electrodes, could be well avoided.

Reproducibility and stability

The as-prepared immunosensor array was stored in dry conditions at 4 °C. In this way, over 90% of the initial response remained intact after 2 weeks of storage. The interassay precision of the immunosensor was examined based on repeated measurements of two different concentrations of CTX with five immunosensors. The coefficient of variation was 4.1%, indicating that the immunosensor has acceptable stability and reproducibility.

Verification by ECLIA

To evaluate the reliability and application potential of the proposed immunoassay, the assay results were compared

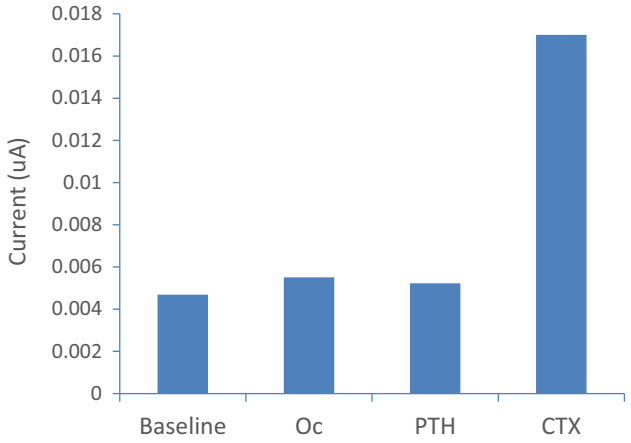

Fig. 6 Response measured for CTX sensor incubated with Osteocalcin (100 pg/mL), PTH (100 pg/mL) and CTX (100 pg/mL)

with the values obtained when testing CTX in human samples by commercial electrochemiluminescent single-analyte tests. In this regard, the serum of seven patients whose CTX levels were recently measured using ECLIA was used. The results are listed in Table 1. Acceptable results with relative errors less than 7.58% indicated good accuracy of the proposed method for real sample analysis.

The correlation between our sensor results and that of ECLIA was also investigated and the results are shown in the correlation and Bland and Altman plots in Fig. 7. The equation of the trendline in the correlation plot has a slope of 0.98 and R^2 of 0.97.

Comparison with existing CTX biosensors

As mentioned earlier in the article, not many sensors were designed to measure CTX levels in serum. Compared to the similar sensors (not optical ones) reported in literature, our method has several advantages and thus would be more compatible for use in point of care (PoC) devices.

- Yun et al. (2009) used bioaffinity immobilization, using avidin and biotin, to immobilize CTX on a self-assembled monolayer and electrochemical impedance spectroscopy (EIS) for the measurement. High cost of proteinaceous-binding reagents and the longer duration of EIS compared with DPV make their label-free electrochemical biosensor less favorable for PoC use. Moreover, the dynamic range of their device was 50–3000 ng/mL; this is while the reference range for

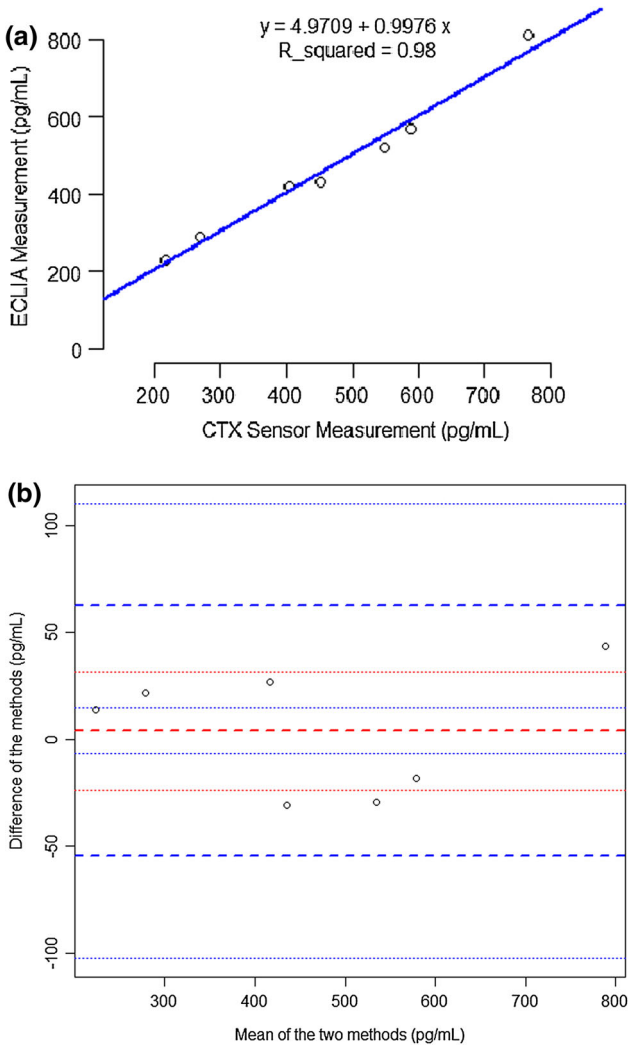

Fig. 7 Statistical analysis comparing ECLIA vs. CTX sensor immunoassay **a** correlation plot **b** bland and Altman plot (Khashayar 2017)

Table 1 Assay results of clinical serum samples using the proposed and reference methods

Serum samples	Proposed method (pg mL^{-1})	Reference method (pg mL^{-1})	Relative error (%)
1	268.02	290	7.58
2	403.13	430	6.25
3	588.43	570	3.23
4	216.38	230	5.92
5	451.03	420	7.39
6	549.55	520	5.68
7	766.34	810	5.39

CTX is 50–450 pg/mL, suggesting that their device had limited use in practice.

- Ramanathan et al. (2016) again used bioafinity immobilization to immobilize CTX on a carbon nanotube array coated with gold nanoparticles. Using EIS as the measurement technique, they managed to achieve a reference range of 0.05–0.6 ng/mL. Despite the fact that they managed to obtain a more clinically applicable dynamic range compared to Yun, their technique was more expensive and less rapid compared with ours.

Conclusion and outlook

In this study, electrochemical detection method was applied to detect serum levels of CTX. AuNPs were electrodeposited on gold electrodes to improve the surface area, provide better electron-transfer kinetics and higher background charging current. On the AuNP-modified gold electrode, CTX antibody was covalently immobilized by crosslinkers and different concentrations of CTX antigen was applied for direct determination. Due to the excellent electrical properties of the as-prepared immunosensor, CTX levels were successfully measured from 1 to 1000 pg/mL. This is while the normal reference of the marker is 50–450 pg/mL, suggesting that the sensor can acceptably detect CTX.

Compared to conventional methods, the proposed electrochemical sensor resulted in selective and sensitive measurement of CTX levels with reduced interference reactions, reduced measurement time, need for less amount of reagent, and better stability in a simplified detection system.

Thus, this highly sensitive label-free CTX sensor showed a potential application for determination of low abundant biomarkers in clinical diagnostics.

Compliance with ethical standards The project was in line with the ethical regulations.

Conflict of interest The authors declare that they have no conflict of interest.

References

Afsarimanesh N, Mukhopadhyay SC, Kruger M (2017) Biosensors for the measurement of C-terminal telopeptide of type I Collagen (CTX-I). Available from: https://www.omicsonline.org/open-access/biosensors-for-the-measurement-of-cterminal-telopeptide-of-type-i-collagen-ctxi-2329-9509-1000199.pdf. Accessed 1 Aug 2017

Baim S, Miller PD (2009) Perspective: assessing the clinical utility of serum CTX in postmenopausal osteoporosis and its use in predicting risk of osteonecrosis of the jaw. J Bone Min Res 24:561–574

Bonde M, Garnero P, Fledelius C, Qvist P, Delmas PD, Christiansen C (1997) Measurement of bone degradation products in serum using antibodies reactive with an isomerized form of an 8 amino acid sequence of the C-telopeptide of type I collagen. J Bone Min Res 12(7):1028–1034

Chubb SAP (2012) Measurement of C-terminal telopeptide of type I collagen (CTX) in serum. Clin Biochem 45(12):928–935

Dhanwal DK, Dennison EM, Harvey NC, Cooper C (2011) Epidemiology of hip fracture: Worldwide geographic variation. Indian J Orthop 45(1):15–22. Available from: http://www.ncbi.nlm.nih.gov/pubmed/21221218. Accessed 14 Dec 2016

Fischer MJ (2010) Amine coupling through EDC/NHS: a practical approach. Methods Mol Biol 627:55–73

Garnero P (2012) The contribution of collagen crosslinks to bone strength. Bonekey Rep 1:182

German N, Ramanavicius A, Ramanaviciene A (2014) Electrochemical deposition of gold nanoparticles on graphite rod for glucose biosensing. Sens Actuat B 203:25–34

Hannon R, Sacco-Gigson N, Mallinak N, Ethgen D, Eastell R (1999) Comparison of ELISA and direct response device to measure urinary type 1 collagen N-telopeptide (NTX) in postmenopausal women. Arth Rheum 42(S9):S290

Heaney RP, Abbott S, Trinkaus E, Burr DB, Aloia JF, Mikhail M et al (2003) Is the paradigm shifting? Bone 33(4):457–465. Available from: http://www.ncbi.nlm.nih.gov/pubmed/14555248. Accessed 14 Dec 2016

Holford TRJ, Davis F, Higson SPJ (2012) Recent trends in antibody based sensors. Biosens Bioelectron 34(1):12–24

Hormozi-Nezhada MR, Seyedhosseinia E, Robatjazia E (2012) Spectrophotometric determination of glutathione and cysteine based on aggregation of colloidal gold nanoparticles. Sci Iran 19(3):958–963

Imai K (2014) Recent methods for assessing osteoporosis and fracture risk. Recent Pat Endocr Metab Immune Drug Discov 8(1):48–59. Available from: http://www.eurekaselect.com/openurl/content.php?genre=article&issn=1872-2148&volume=8&issue=1&spage=48. Accessed 14 Dec 2016

Johnell O, Kanis JA (2006) An estimate of the worldwide prevalence and disability associated with osteoporotic fractures. Osteoporos Int 17(12):1726–1733. doi:10.1007/s00198-006-0172-4

Khashayar P, Aghaei Meybodi HR, Homami MR, Heshmat R, Larijani B (2010) The prevalence of osteoporosis in an Iranian population. J Clin Densitom 13(1):112. Available from: http://linkinghub.elsevier.com/retrieve/pii/S1094695010000235. Accessed 4 Nov 2016

Khashayar P, Aghaei Meybodi H, Amoabediny G, Larijani B (2015) Biochemical markers of bone turnover and their role in osteoporosis diagnosis: a narrative review. Recent Pat Endocr Metab Immune Drug Discov 9(2):79–89

Khashayar P, Amoabediny G, Schaubroeck D, De Keersmaecker M (2016) Characterization of gold nanoparticle layer deposited on gold electrode by various techniques. Biointerface Res Appl Chem 6(4):1380–1390

Khashayar P (2017) Oc and CTX BioSensors: characteristics and validation. In: Point-of-Care solution for osteoporosis management: design, fabrication, and validation of new technology [Internet]. Springer International Publishing, Cham, pp 127–151

Killard AJ, Deasy B, O'Kennedy R, Smyth MR (1995) Antibodies: production, functions and applications in biosensors. Trends Anal Chem 14(6):257–266

Kim SJ, Park YM, Min B-H, Lee D-S, Yoon HC (2013) Optical immunosensor for quantifying C-telopeptide fragments of type II collagen as an osteoarthritis biomarker in urine. BioChip J 7(4):399–407. doi:10.1007/s13206-013-7412-4

La Belle JT, Fairchild A, Demirok UK, Verma A (2013) Method for fabrication and verification of conjugated nanoparticle-Ab tuning elements for multiplexed electrochemical biosensors. Methods 61(1):39–51

Nishizawa Y, Ohta H, Miura M, Inaba M, Ichimura S, Shiraki M et al (2012) Guidelines for the use of bone metabolic markers in the diagnosis and treatment of osteoporosis. J Bone Miner Metab 31(1):1–15. doi:10.1007/s00774-012-0392-y

Omidfar K, Khorsand F, Darziani AM (2013) New analytical applications of gold nanoparticles as label in Ab based sensors. Biosens Bioelectron 43:336–347

Park YM, Kim SJ, Lee KJ, Yang SS, Min B-H, Yoon HC (2015) Detection of CTX-II in serum and urine to diagnose osteoarthritis by using a fluoro-microbeads guiding chip. Biosens Bioelectron 67:192–199. http://linkinghub.elsevier.com/retrieve/pii/S0956566314006046. Accessed 1 Aug 2017

Ramanathan M, Patil M, Epur R, Yun Y, Shanov V, Schulz M et al (2016) Gold-coated carbon nanotube electrode arrays: immunosensors for impedimetric detection of bone biomarkers. Biosens Bioelectron 77:580–588

Reverberi R, Reverberi L (2007) Factors affecting the Ag-Ab reaction. Blood Transfus 5(4):227–240

Rosenquist C, Fledelius C, Christgau S, Pedersen BJ, Bonde M, Qvist P et al (1998) Serum CrossLaps One Step ELISA. First application of monoclonal antibodies for measurement in serum of bone-related degradation products from C-terminal telopeptides of type I collagen. Clin Chem 44(11):2281–2289

Shamsipur M, Saber R, Emami M (2014) A highly sensitive electrochemical sensor based on gold nanoparticles/multiwall carbon nanotubes-modified glassy carbon electrode for selective determination of traces of atenolol. Anal Methods. 6(17):7038. http://xlink.rsc.org/?DOI=C4AY01538J. Accessed 4 Nov 2016

Sornay-Rendu E, Munoz F, Garnero P, Duboeuf F, Delmas PD (2005) Identification of osteopenic women at high risk of fracture: the OFELY study. J Bone Miner Res 20(10):1813–1819. doi:10.1359/JBMR.050609

Srivastava AK, Vliet EL, Michael Lewiecki E, Maricic M, Abdelmalek A, Gluck O et al (2005) Clinical use of serum and urine bone markers in the management of osteoporosis. Curr Med Res Opin 21(7):1015–1026. doi:10.1185/030079905X49635

Svedbom A, Hernlund E, Ivergård M, Compston J, Cooper C, Stenmark J et al (2013) Osteoporosis in the European Union: a compendium of country-specific reports, vol 8. Archives of Osteoporosis, London

Uludag Y, Olcer Z, Sagiroglu MS (2014) Design and characterization of a thin-film electrode array with shared reference/counter electrodes for electrochemical detection. Biosens Bioelectron 57:85–90

Vasikaran S, Cooper C, Eastell R, Griesmacher A, Morris HA, Trenti T et al (2011) International Osteoporosis Foundation and International Federation of Clinical Chemistry and Laboratory Medicine Position on bone marker standards in osteoporosis. Clin Chem Lab Med

Vastarella W, Della Seta L, Masci A, Maly J, De Leo M, Maria Moretto L et al (2007) Biosensors based on gold nanoelectrode ensembles and screenprinted electrodes. Int J Environ Anal Chem 87(10–11):701–714

Wang J (2006) Electrochemical biosensors: towards point-of-care cancer diagnostics. Biosens Bioelectron 21(10):1887–1892

Yun Y-H, Bhattacharya A, Watts NB, Schulz MJ (2009) A label-free electronic biosensor for detection of bone turnover markers. Sensors 9:7957–7969. Available from: http://www.mdpi.com/journal/sensors